PHYSICAL REVIEW D **93,** 126001 (2016)

Lifshitz scaling effects on the holographic paramagnetism-ferromagnetism phase transition

Cheng-Yuan Zhang,[1] Ya-Bo Wu,[1,*] Yong-Yi Jin,[2] Yun-Tian Chai,[1] Mu-Hong Hu,[1] and Zhuo Zhang[1]

[1]*Department of physics, Liaoning Normal University, Dalian 116029, China*

[2]*China criminal police University, Shenyang 110035, China*

(Received 14 March 2016; published 6 June 2016)

In the probe limit, we investigate holographic paramagnetism-ferromagnetism phase transition in the four-dimensional and five-dimensional Lifshitz black holes by means of numerical and semianalytical methods, which is realized by introducing a massive 2-form field coupled to the Maxwell field. We find that the Lifshitz dynamical exponent z contributes evidently to the magnetic moment and hysteresis loop of single magnetic domain quantitatively, not qualitatively. Concretely, in the case without an external magnetic field, the spontaneous magnetization and ferromagnetic phase transition happen when the temperature gets low enough, and the critical exponent for the magnetic moment is always $1/2$, which is in agreement with the result from mean field theory. And the increasing z enhances the phase transition and increases the dc resistivity, which behaves as the colossal magnetic resistance effect in some materials. Furthermore, in the presence of the external magnetic field, the magnetic susceptibility satisfies the Cure-Weiss law with a general z. But the increase of z will result in shortening the period of the external magnetic field.

DOI: 10.1103/PhysRevD.93.126001

I. INTRODUCTION

The AdS/CFT correspondence [1–4] provides a window into the dynamics of strongly coupled systems by identifying the underlying field theory with a weakly coupled gravity dual. Because of the existence of scaling symmetry near the critical point, over the past years, the methods and scope of the gauge/gravity have shifted from traditionally QCD-motivated problems to problems in the area of condensed matter systems (see reviews [5–8] and references therein) involving the strong interaction. And the duality also gives us a way to understand gravity and condensed matter physics from the other side.

One interesting application of the duality is to study high-temperature superconductors, and then several models of holographic s-wave [9,10] and p-wave superconductors [11,12] have been constructed among the various paradigms in condensed matter physics. For example, the holographic s-wave superconductor model was first realized via an Einstein-Maxwell theory coupled to a complex scalar field in a Schwarzschild–anti-de Sitter (AdS) black hole background [9,13–15]. The condensation of the scalar breaks the U(1) symmetry of the system, mimicking the conductor-superconductor phase transition. Sequentially, one analytically studied the superconductor phase transition near the critical point [16]. Moreover, by an SU(2) gauge field in the bulk, a holographic p-wave superconductor model was constructed [12], in which the condensed vector field breaks the U(1) symmetry [one of subgroup of SU(2)] as well as the spatial rotational symmetry spontaneously.

Recently, some efforts have been made to generalize the correspondence to systems with fewer symmetries (see Refs. [16–22], for example) and to the far-from-thermal equilibrium problems (see Refs. [23–27], for example).

The other application of duality is to study ferromagnetism where the electron spins align to produce a magnetization, which breaks the time reversal symmetry spontaneously and happens in the ferromagnets at the Curie temperature T_c (sometimes, it is even higher than the indoor temperature). As we know, magnetism plays a central role in quantum phase transitions and is ubiquitous in many strongly correlated electronic systems, for example, heavy fermion metals. Yet in holographic contexts, due to various technical challenges, models of magnetism are scarce and not extensively explored (see, e.g., Ref. [28]).

In Ref. [29], a new example of the application of the AdS/CFT correspondence was proposed at first to understand these challenging systems by realizing the holographic description of the paramagnetism-ferromagnetism phase transition in a dyonic Reissner-Nordström-AdS black brane. In that model, the magnetic moment is realized by the condensation of a real antisymmetric tensor field which couples to the background gauge field strength in the bulk. In the case without an external magnetic field, the time reversal symmetry is spontaneously broken, and the spontaneous magnetization happens in low temperatures. The critical exponents are in agreement with the ones from mean field theory. In the case of a nonzero magnetic field, the model realizes the hysteresis loop of the single magnetic domain, and the magnetic susceptibility satisfies

*ybwu61@163.com

the Curie-Weiss law. Obviously, this model in Ref. [29] gives a good starting point to explore more complicated magnetic phenomena and quantum phase transitions.

Although a real antisymmetric tensor field was introduced to realize a holographic magnetic ordered phase in the above model, a more careful analysis shows there is a vector ghost in the model. Hence, in Ref. [30], a modified Lagrangian density was put forward; it comes from the dimensional compactification of p-form field in string/M-theory for the antisymmetric tensor, which is ghost free and in which causality is well defined, and keeps all the significant results in the original model qualitatively.

On the basis of Ref. [29], the model was further extended to realize a holographic model of paramagnetism-antiferromagnetism phase transition by introducing two real antisymmetric tensor fields coupling to the background gauge field strength and interacting with each other [31]. And then one studied the coexistence and competition of ferromagnetism and p-wave superconductivity by combining a holographic p-wave superconductor model with a holographic ferromagnetism model [32]. It was found that the results in Ref. [32] depend on the phase appearing first (superconductivity or ferromagnetism) besides the self-interaction of the magnetic moment of the complex vector field.

On the other hand, for insulator-metal phase transition, a gravity duality model was constructed by introducing a massive 2-form field and a dilaton field coupled with U(1) gauge field in an asymptotic AdS black brane background. This model shows the colossal magnetoresistance (CMR) effect found in some manganese oxides materials [33]. Further studies based on this model can be discovered, for example, the effect of backreaction on the holographic paramagnetism/ferromagnetism. In Ref. [34], one found that the phase transition is always second order, which is different from holographic superconductor exhibiting rich phase structures, especially "the retrograde condensate." At present, the holographic duality has been applied to two-dimensional magnetic systems [28,29,34], where the behaviors near the critical temperature were discussed. However, the setup in Ref. [35] deals with three-dimensional magnetic systems and describes their behaviors in low temperatures where the technology of spintronics is actively developed, besides near the critical temperature. This holographic model in principle can provide a means to analyze phenomena involving magnetization and spin transport, and thus it can introduce new perspectives in the field of spintronics. However, all these holographic ferromagnetic models were constructed only in the relativistic spacetimes. Thus, we wonder whether the above results still hold in nonrelativistic spacetimes, for example, the Lifshitz spacetime, which is our motivation in this paper.

This paper is organized as follows. In Sec. II, we build a holographic paramagnetism-ferromagnetism phase transition model in the Lifshitz black hole with AdS_2 geometry, which is realized by introducing a massive 2-form field coupled to the Maxwell field strength in the bulk. In Sec. III, by the semianalytic method, we study the magnetic moment and static magnetic susceptibility. The summary and some discussions are included in Sec. IV.

II. HOLOGRAPHIC MODEL

A. Background

Recently, the phase transitions in many condensed matter systems have been found to be governed by the so-called Lifshitz fixed points, which exhibit the anisotropic scaling of spacetime $t \to b^z t$, $\vec{x} \to b\vec{x}$ $(z \neq 1)$, where z is the Lifshitz dynamical exponent representing the anisotropy of the spacetime. The gravity description dual to this scaling in the $D = d + 2$-dimensional spacetime was proposed in Ref. [36],

$$ds^2 = L^2\left(-r^{2z}dt^2 + r^2 d\vec{x}^2 + \frac{dr^2}{r^2}\right), \qquad (1)$$

where $d\vec{x}^2 = dx_1^2 + \cdots + dx_d^2$, and $r \in (0, \infty)$. This geometry reduces to the AdS spacetime when $z = 1$, while it is a gravity dual with the Lifshitz scaling as $z > 1$. The Lifshitz spacetime (1) can be realized by a massless scalar field coupled to an Abelian gauge field in the action [37]

$$S = \frac{1}{16\pi G_{d+2}} \int d^{d+2}x\sqrt{-g}\Big(R - 2\Lambda - \frac{1}{2}\partial_\mu\varphi\partial^\mu\varphi - \frac{1}{4}e^{b\varphi}F_{\mu\nu}F^{\mu\nu}\Big), \qquad (2)$$

where Λ is the cosmological constant, φ is a massless scalar, and $F_{\mu\nu}$ is an Abelian gauge field strength. The generalization of Eq. (1) to the case with finite temperature is [38]

$$ds^2 = L^2\left(-r^{2z}f(r)dt^2 + \frac{dr^2}{r^2 f(r)} + r^2\sum_{i=1}^{d}dx_i^2\right), \qquad (3)$$

where

$$f(r) = 1 - \frac{r_h^{z+d}}{r^{z+d}}, \quad \Lambda = -\frac{(z+d-1)(z+d)}{2L^2}, \qquad (4)$$

$$\mathcal{F}_{rt} = q_0 r^{z+d-1}, \qquad q_0^2 = 2L^2(z-1)(z+d),$$
$$e^{b\varphi} = r^{-2d}, \qquad b^2 = \frac{2d}{z-1}. \qquad (5)$$

Evidently, choosing the dynamical exponent z to be 1 reduces the Lifshitz black hole to the Schwarzschild AdS black hole in $(d + 2)$ dimensions. The Hawking temperature of the black hole is

$$T = \frac{z+d}{4\pi} r_h^z, \tag{6}$$

where r_h denotes the black hole horizon. As we know, some works have been carried out for the influence of the dynamical critical exponent on the properties of holographic superconductors (for details, see Ref. [39–45]). For example, Refs. [39] and [40], studied the scalar condensation in a $(3+1)$-dimensional Lifshitz black hole background with $z = 3/2$ and $z = 2$, respectively. The s-wave and p-wave superconductor models were built in the $(3+1)$-dimensional Lifshitz black hole with $z = 2$ [41]. Recently, Abdalla *et al.* in Ref. [43] investigated the s-wave superconductor phase transition in a three-dimensional Lifshitz black hole in new massive gravity with $z = 3$ and found a series of peaks in the conductivity for certain values of the frequency. Based on the previous investigation on the Lifshitz black hole solution, the effects of the Lifshitz dynamical exponent z on the holographic superconductor models were discussed in some detail via numerical and analytical methods, including s-wave and p-wave models with [46] or without magnetic field [47] [46]. Therefore, it is interesting to construct a holographic ferromagnetic phase transition by using Lifshitz black hole solutions and to study the influences of the dynamical exponent z on the properties of the holographic ferromagnetic phase transition and colossal magnetoresistance effect.

B. Model and EoMs

Following Ref. [30], below, we consider the Lagrangian density consisting of a U(1) field A_μ and a massive 2-form field $M_{\mu\nu}$ in $(d+2)$-dimensional spacetime,

$$\mathcal{L}_m = -F^{\mu\nu}F_{\mu\nu} - \lambda^2\left(\frac{1}{12}(dM)^2 + \frac{m^2}{4}M_{\mu\nu}M^{\mu\nu} + \frac{1}{2}M^{\mu\nu}F_{\mu\nu} + \frac{J}{8}V(M)\right), \tag{7}$$

where dM is the exterior differential of 2-form field $M_{\mu\nu}$, m^2 is the squared mass of 2-form field $M_{\mu\nu}$ being greater than zero (see Ref. [30] for details), λ and J are two real model parameters with $J < 0$ for producing the spontaneous magnetization, λ^2 characterizes the backreaction of the 2-form field $M_{\mu\nu}$ to the background geometry and to the Maxwell field strength, and $V(M)$ is a nonlinear potential of the 2-form field describing the self-interaction of the polarization tensor. For simplicity, we take the form of $V(M)$ as

$$V(M) = ({}^*M_{\mu\nu}M^{\mu\nu})^2 = [{}^*(M\wedge M)]^2, \tag{8}$$

where $*$ is the Hodge-star operator. As shown in Ref. [30], this potential shows a global minimum at some nonzero value of ρ.

By varying action (7), we can get the equations of motion (EoMs) for the matter fields as

$$\nabla^\tau(dM)_{\tau\mu\nu} - m^2 M_{\mu\nu} - J({}^*M_{\tau\sigma}M^{\tau\sigma})({}^*M_{\mu\nu}) = F_{\mu\nu},$$
$$\nabla^\mu\left(F_{\mu\nu} + \frac{\lambda^2}{4}M_{\mu\nu}\right) = 0. \tag{9}$$

In what follows, we start to study systematically the effects of the Lifshitz dynamical exponent z on the holographic ferromagnetic phase transition based on the Lifshitz spacetime (3) in the probe limit (i.e., neglecting the backreactions of the massive 2-form field to the background Lifshitz geometry and Maxwell field, also including the Maxwell field to the background geometry). In this probe approximation, the interaction between the electromagnetic response and external field is taken into account so that we can study how spontaneous magnetization influences the electric transport in the following, but they both have little influence on the structures of materials. We take the self-consistent ansatz with matter fields,

$$M_{\mu\nu} = -p(r)dt\wedge dr + \rho(r)dx\wedge dy,$$
$$A_\mu = \phi(r)dt + Bxdy, \tag{10}$$

where B is a constant magnetic field viewed as the external magnetic field in the boundary field theory. Thus, nontrivial equations of motion in $\mathrm{D} = d+2$-dimensional Lifshitz spacetime read

$$\rho'' + \left(\frac{f'}{f} + \frac{d+z-3}{r}\right)\rho' - \frac{1}{r^2 f}\left[m^2 + \frac{4Jp^2}{r^{2z-2}}\right]\rho + \frac{B}{r^2 f} = 0,$$
$$\left(m^2 - \frac{4J\rho^2}{r^4}\right)p - \phi' = 0,$$
$$\phi'' + \frac{d-z+1}{r}\phi' - \lambda^2\left(\frac{p'}{4} + \frac{(d+1)p}{4r} - \frac{pz}{4r}\right) = 0, \tag{11}$$

where a prime stands for the derivative with respect to r. To solve the above equations, we have to specify boundary conditions for the fields. At the horizon $r \to r_h$, we impose $\phi(r_h) = 0$ to satisfy the finite form A_μ, while $\rho(r_h)$ needs to be regular. Near the boundary $r \to \infty$, the linearized equations give the asymptotic solution for matter fields,

$$\rho = \rho_+ r^{\Delta_+} + \rho_- r^{\Delta_-} + \cdots + \frac{B}{m^2},$$
$$\phi = \mu - \frac{\sigma}{r^{(d-z)}} + \ldots,\ p = \frac{\sigma(d-z)}{m^2 r^{d-z+1}} + \ldots,\ (z \neq d)$$
$$\phi = \mu + \sigma \ln r + \ldots,\ p = \frac{\sigma}{rm^2} + \ldots.(z = d), \tag{12}$$

where $\Delta_\pm = \frac{4-d-z\pm\sqrt{4(m^2+4)+(d+z)(d+z-8)}}{2}$ and $\rho_\pm$, μ, and σ are all constants. According to gauge-gravity duality and the explanation for the source in Ref. [30], we treat ρ_+ as the source of the dual operator, namely, $\rho_+ = 0$, and μ and σ are chemical potential and charge density of dual field theory, respectively.

The Breitenlohner-Freedmeltaan (BF) bound requires $m^2 \geq \frac{-(d+z)(d+z-8)}{4} - 4$, and the mass squared m^2 of massive 2-form field has the lower bound. In this case, there is a logarithmic term in the asymptotical expansion (12). We treat the coefficient of this logarithmic term as the source which is set to be zero to avoid the instability induced by this term according to Ref. [13]. Within the BF bound condition, there does not exist the AdS_2 geometry and the near horizon geometry of an extremal black brane with vanishing temperature. To find the restriction to the parameters, let us consider Eqs. (11) in the high-temperature region where ρ vanishes, and we can read off the effective mass square of ρ at the horizon as

$$\begin{aligned} m_{\rm eff}^2 &= m^2 + 4Jp(r_h)^2 \\ &= m^2 + \frac{4J\mu^2(d-z)^2}{m^4 r_h^{2d}} \\ &= m^2 + \frac{4J\mu^2(d-z)^2}{m^4}\left(\frac{z+d}{4\pi T}\right)^{\frac{2d}{z}}. \end{aligned} \tag{13}$$

Because $J < 0$, the temperature term contributes a negative term to the effective mass square, which is divergent when $T \to 0$. It follows that, whether we choose the grand canonical ensemble or the canonical ensemble, the instability always appears provided that the temperature is low enough.

C. Spontaneous magnetization and susceptibility

In this paper, we consider the canonical ensemble where the charge density σ will be fixed when we discuss the Lifshitz black hole background. Concretely, we first consider the cases of $z = 1$ and 2 in the four-dimensional (4D) spacetime as examples by the numerical and analytic methods and then extend to the cases of $z = 1$, 2, and 3 in the five-dimensional (5D) spacetime. Now, we think about the spontaneous magnetization in this probe approximation in the 4D spacetime. To begin with, we compute the critical temperature T_c when $B = 0$. Similar to the case in the Ref. [30], the polarization field ρ is a small quantity near the critical temperature, and we can neglect the nonlinear terms of ρ in the equations of ϕ and p. Then, we can get

$$\begin{aligned} &\phi(r) = \mu\left(1 - \frac{1}{r^{2-z}}\right), \qquad p(r) = \frac{\mu(2-z)}{m^2 r^{3-z}}, \quad (z \neq d), \\ &\phi(r) = \mu \ln r, \qquad p(r) = \frac{\mu}{m^2 r}. \quad (z = d). \end{aligned} \tag{14}$$

In the following calculations, we will consider these two cases of $z \neq d$ and $z = d$. Then, the equations of ρ are as follows:

$$\begin{aligned} &\rho'' + \left(\frac{f'}{f} + \frac{z-1}{r}\right)\rho' - \frac{1}{r^2 f}\left[m^2 + \frac{4J\mu^2(2-z)^2}{m^4 r^4}\right]\rho = 0, \ (z \neq d), \\ &\rho'' + \left(\frac{f'}{f} + \frac{1}{r}\right)\rho' - \frac{1}{r^2 f}\left[m^2 + \frac{4J\mu^2}{m^4 r^4}\right]\rho = 0. \ (z = d). \end{aligned} \tag{15}$$

To find the critical temperature, at the horizon, the initial conditions are

$$\begin{aligned} &\rho' = \frac{m^6 + 4J\mu^2 z^2 - 16J\mu^2(1-z)}{(z+2)m^4}, \qquad \rho(r_h) = 1. \quad (z \neq d) \\ &\rho' = \frac{m^6 + 4J\mu^2}{4m^4}, \qquad \rho(r_h) = 1. \quad (z = d). \end{aligned} \tag{16}$$

When we perform the numerical computation, we can first fix the horizon radius $r_h = 1$, and thus the temperature is also fixed. Without loss of generality, we take $\rho(r_h) = 1$ and treat the chemical potential μ as the shooting parameter to match the boundary condition $\rho_+ = 0$. And then we can use the scaling transformations to transform our results into the case in canonical ensemble where the charge density is fixed. As a typical example, we also choose parameters as $m^2 = -J = 1/8$ and $\lambda = 1/2$. Thus, the critical temperature T_c will be found and is listed in Table I. When the temperature is lower than the critical temperature, we can plot the relationship between ρ_+ and the shooting parameter μ, in order to examine whether ρ gets spontaneous condensation. We find that the solution of source free always appears, which results in the spontaneous magnetization of the system and breaks the time reversal symmetry in low temperatures. In addition, here, it is worth stressing that in the 5D spacetime the spatial rotational symmetry is also broken spontaneously, since a nonvanishing magnetic moment chooses a direction as a special. When the temperature is lower than the critical one T_c, we have to solve Eq. (11) to get the solution of the order parameter ρ and then compute the value of magnetic moment N, which is defined in the 4D spacetime by

$$N = -\lambda^2 \int \frac{\rho}{2r^{3-z}} dr. \tag{17}$$

Figure 1 shows the value of magnetic moment N as a function of temperature with various z in 4D and 5D Lifshitz black holes backgrounds. Here, in order to see clearly the effect of the dynamical critical exponent z on paramagnetism-ferromagnetism phase transition, we fix the mass squared m^2 of the massive 2-form field. We see that when the temperature is lower than T_c the nontrivial solution $\rho \neq 0$ and the spontaneous magnetic moment

TABLE I. The critical temperature, magnetic moment, and static magnetic susceptibility for the paramagnetic-ferromagnetic phase transition in Lifshitz black hole backgrounds. Here, $t = 1 - T/T_c$, and the subscript SL denotes the quantity calculated by the semianalytic method. $N_{c;SL}/\lambda^2\sigma^{z/d}$, $\lambda^2/\chi_{c;SL}\sigma^{z/d}$, $N/\lambda^2\sigma^{z/d}$, and $\lambda^2/\chi\sigma^{z/d}$ are calculated near T_c. Here, each coefficient from $C1$ to γ should be multiplied by 10^2 for the case of $z = 2$ in 5D spacetime, but the order of magnitude when we take $z = 3$ in 5D spacetime is 10^7.

D	z	k	$C1$	$N1$	$a1$	$a0$	$\gamma 1$	$\frac{N_{c;SL}}{\lambda^2\sigma^{z/d}}$	$\frac{\lambda^2}{\chi_{c;SL}\sigma^{z/d}}$	$\frac{N}{\lambda^2\sigma^{z/d}}$	$\frac{\lambda^2}{\chi\sigma^{z/d}}$	$T_c/\sigma^{z/d}$
4	1	3	0.234	1.837	0.477	1.849	1.838	$1.341t^{1/2}$	$-2.996t$	$1.332t^{1/2}$	$-2.966t$	0.653
4	1	4	0.189	2.042	0.727	2.284	2.042	$1.341t^{1/2}$	$-2.996t$			
4	2	3	0.212	5.900	0.588	3.078	6.136	$19.218t^{1/2}$	$-0.170t$	$19.27t^{1/2}$	$-0.57t$	1.451
4	2	4	0.175	6.496	0.864	3.732	6.757	$19.218t^{1/2}$	$-0.170t$			
5	1	3	0.203	5.757	0.504	9.273	5.987	$32.913t^{1/2}$	$-0.538t$	$19.09t^{1/2}$	$-0.508t$	0.627
5	1	4	0.169	6.325	0.734	11.191	6.577	$32.913t^{1/2}$	$-0.538t$			
5	2	3	0.002	0.139	0.007	0.171	0.215	$25.468t^{1/2}$	$-0.088t$	$13.692t^{1/2}$	$-0.05t$	0.674
5	2	4	0.001	0.149	0.010	0.198	0.231	$25.468t^{1/2}$	$-0.088t$			
5	3	3	…	…	…	…	…	$21.823t^{1/2}$	$-0.039t$	$744.075t^{1/2}$	$-0.95t$	0.764
5	3	4	…	…	…	…	…	$21.823t^{1/2}$	$-0.039t$			

appears. The numerical results show that this phase transition is a second-order one with the behavior $N \propto \sqrt{1 - T/T_c}$ near the critical temperature for all cases calculated above. The result is still consistent with one in the mean field theory describing the paramagnetism-ferromagnetism phase transition. Note that when taking $z = 1$ and 2 in the 4D and 5D cases the magnetic moment will decrease with the increasing z; for instance, for the case of $z = 2$ in 4D, the value of the magnetic moment is smaller than the other ones in 4D. However, from the lower right corner of Fig. 1, it easy to see that the magnetic moment increases faster when $T < T_c$ than those of other curves in the 5D case. This might be due to the fact that for the cases of $z = 2$ in 4D spacetime and $z = 3$ in 5D spacetime there is a logarithmic term in the expansion of the gauge field ϕ near the boundary $r \to \infty$. In addition, at the sufficient low temperature, the backreaction effect of the matter sector on the background geometry becomes important, and thus the probe approximation considered here would be no longer valid.

For comparison, we list in Table I the critical temperature T_c and the condensation behavior near T_c for the cases of $z = 1$, 2, and 3 with the fixed squared mass. From the table, we can find that when we increase z T_c increases for the fixed D, which indicates that the increasing anisotropy between space and time enhances the phase transition. This can be understood as follows. We can see from Eqs. (11) that near the horizon the effective mass of the massive 2-form field decreases as the dynamical critical exponent z increases. This leads to a higher critical temperature as z increases. And the instability of the massive 2-form field is easier to implement.

In the following, we calculate the static magnetic susceptibility in this probe limit, defined by

$$\chi = \lim_{B\to 0} \frac{\partial N}{\partial B}. \tag{18}$$

Based on the previous analysis [30], the magnetic susceptibility is still obtained by solving

$$\rho'' + \left(\frac{f'}{f} + \frac{z-1}{r}\right)\rho' - \frac{1}{r^2 f}\left[m^2 + \frac{4J\mu^2(2-z)^2}{m^4 r^4}\right]\rho + \frac{B}{r^2 f} = 0 (z \neq d),$$
$$\rho'' + \left(\frac{f'}{f} + \frac{z-1}{r}\right)\rho' - \frac{1}{r^2 f}\left[m^2 + \frac{4J\mu^2}{m^4 r^4}\right]\rho + \frac{B}{r^2 f} = 0 (z = d). \tag{19}$$

Thus, when setting the magnetic field $B = 1$, we can get $\frac{\lambda^2}{\chi\sqrt{\sigma}} = 2.966(T/T_c - 1)$ and $\frac{\lambda^2}{\chi\sigma} = 0.5751(T/T_c - 1)$ for the cases of $z = 1$ and 2 in 4D spacetime, respectively. And they all satisfy the Curie-Weiss law of ferromagnetism in the region of $T > T_c$. This conclusion is similar to the one in the 5D case. The inverse susceptibility density in paramagnetic phase is shown in Fig. 2.

D. DC conductivity in the ferromagnetic phase

As we know, the electric transport is also an important property in the materials involving spontaneous magnetization. Now, let us study how the dc conductivity is influenced by spontaneous magnetization in this model. To simplify our computation in technology, we will work in the probe limit by neglecting backreactions of all the matter

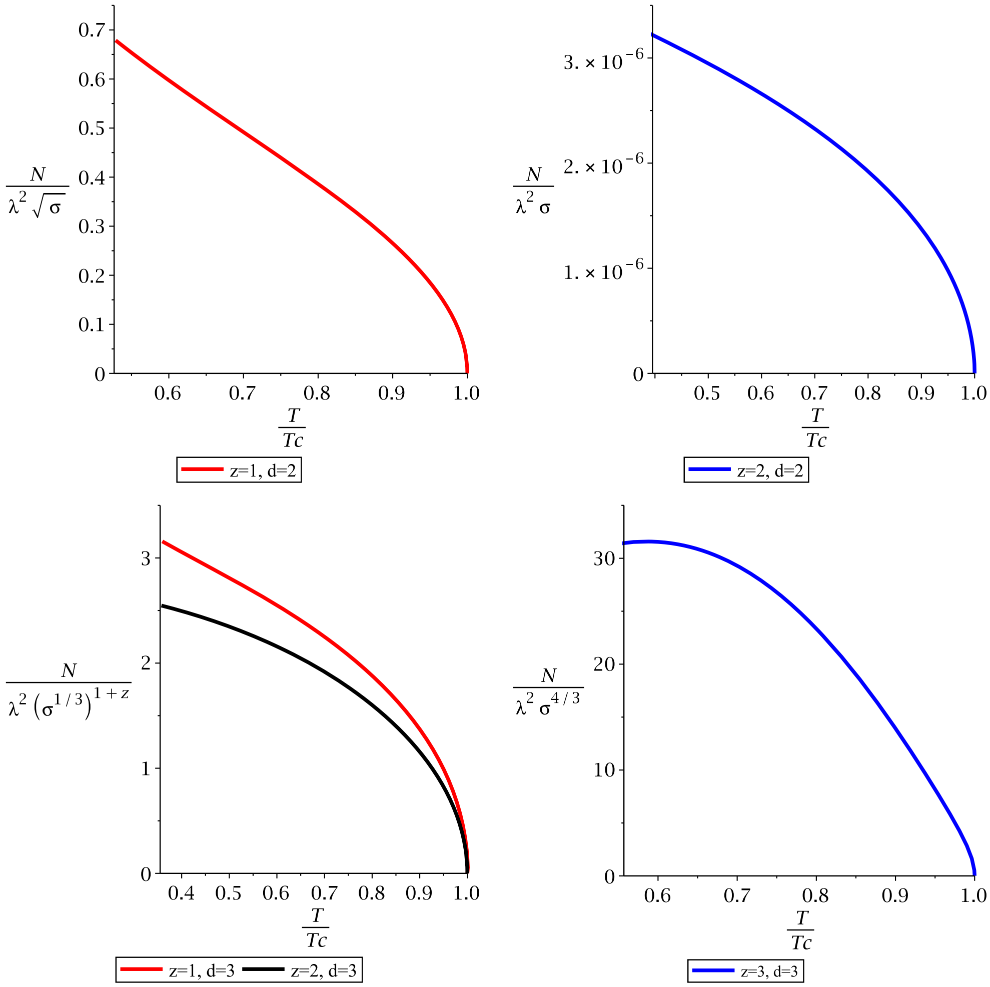

FIG. 1. The magnetic moment N as a function of temperature. Top panel: The corresponding temperatures $T_c/\sqrt{\sigma} \simeq 0.6532$ and $T_c/\sigma \simeq 1.4514$ to $z = 1$ and 2 in the 4D case, respectively. Bottom panel: The corresponding temperatures $T_c/\sigma^{1/3} \simeq 0.6274$, $T_c/\sigma^{2/3} \simeq 0.6738$, and $T_c/\sigma \simeq 0.7642$ to $z = 1$, 2, and 3 in the 5D case, respectively.

fields. This limit can give out the main features near the critical temperature. However, in the case of near-zero temperature, we have to consider the model with full backreaction, which will be our work in the near future.

To compute the conductivity, we have to consider some perturbations for the gauge field with a harmonically time varying electric field. Because of the planar symmetry at the boundary, the conductivity is isotropic. Thus, for simplicity, we just compute the conductivity along the x direction. According to the dictionary of AdS/CFT, we consider the perturbation $\delta A_x = \epsilon a_x(r) e^{-i\omega t}$. In the probe limit, this perturbation will also lead to the perturbations of the polarization field in the first order of ϵ. As a result, we have to consider the perturbations for all the components of the gauge field and polarization field. However, if we only care about the conductivity in the low-frequency limit, i.e., $T \gg \omega \to 0$, the problem can be simplified. In the low-frequency limit, we only need turn on the three perturbations,

$$\begin{aligned} \delta A_x &= \epsilon a_x(r) e^{-i\omega t}, \\ M_{rx} &= \epsilon C_{rx}(r) e^{-i\omega t}, \\ M_{ty} &= \epsilon C_{ty}(r) e^{-i\omega t}, \end{aligned} \tag{20}$$

and corresponding equations to the three perturbations in the low-frequency limit with Lifshitz scaling z read

$$C''_{ty} + \left(\frac{1-z}{r}\right) C'_{ty} - \frac{m^2 C_{ty}}{r^2 f} - \frac{4Jp\rho C_{rx}}{r^2} + O(\omega) = 0, \tag{21a}$$

$$C_{rx} - \frac{a'_x}{m^2} - \frac{4Jp\rho C_{ty}}{r^{2z+2} f m^2} + O(\omega) = 0, \tag{21b}$$

$$[r^{z+1} f(a'_x - \lambda^2 C_{rx}/4)]' + \frac{a_x \omega^2}{r^{z+1} f} + O(\omega) = 0, \tag{21c}$$

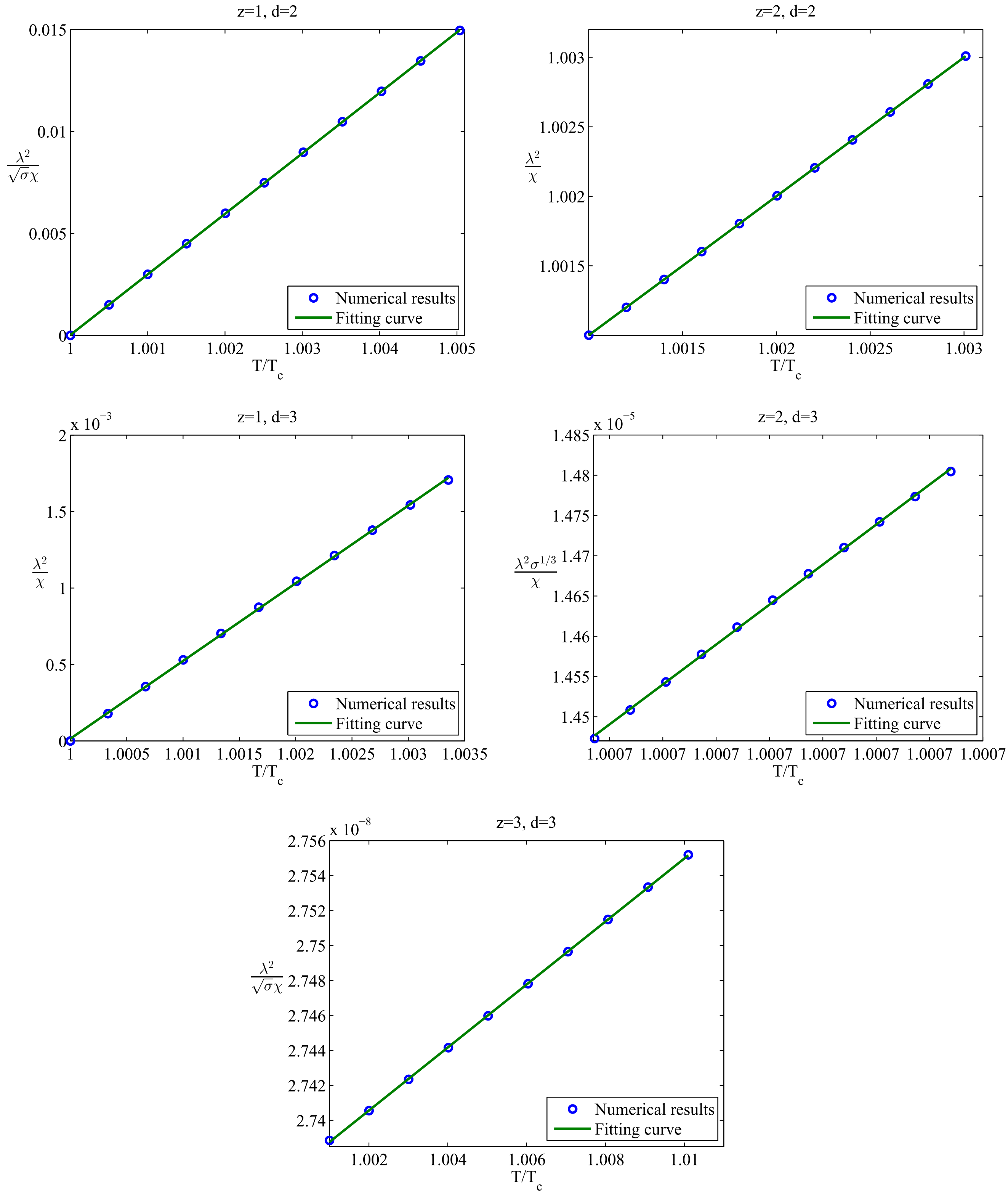

FIG. 2. The behavior of the inverse susceptibility density in the paramagnetic phase near the critical temperature when $m^2 = -J = 1/8$. Here, we set $2\kappa^2 = 1$ for convenience. Top panel: $z = 1$ and 2 in the 4D case from left to right. Bottom panel: $z = 1$, 2, and 3 in the 5D case from left to right.

with p and ρ determined by Eqs. (11). Here, $O(\omega)$ is the terms with order of ω which can be neglected when $\omega \to 0$. In general, the term $\omega^2/r^{z+1}f(r)$ cannot be neglected since $f(r)$ is zero at the horizon, which makes the limit of $\omega \to 0$ ambiguous. However, at the horizon, if we impose the ingoing conditions for C_{rx}, C_{ty}, and a_x,

$$\begin{aligned} C_{ty} &= e^{-i\omega r_*}[C_{ty}^{(0)} + C_{ty}^{(1)}(r - r_h) + \ldots], \\ C_{rx} &= e^{-i\omega r_*}[C_{rx}^{(0)} + C_{rx}^{(1)}(r - r_h) + \ldots], \\ a_x &= e^{-i\omega r_*}[a_x^{(0)} + a_x^{(1)}(r - r_h) + \ldots], \end{aligned} \tag{22}$$

with $r_* = \int dr/(r^{z+1}f)$, we find the system has a well-defined limit when $\omega \to 0$ if $T \neq 0$. At the AdS boundary with the source free condition, we have the following asymptotic solutions:

$$\begin{aligned} C_{ty} &= C_{ty+}r^{(z+\delta)/2} + C_{ty-}r^{(z-\delta)/2} + \ldots, \\ C_{rx} &= -\frac{z a_{x-}}{r^{z+1}m^2} + \ldots, \\ a_x &= a_{x+} + \frac{a_{x-}}{r^z} + \ldots. \end{aligned} \tag{23}$$

Here, $\delta = \sqrt{4m^2 + z^2}$. Then, the gauge-gravity duality implies that the electric current $\langle J_x \rangle = a_{x-}$ and the dc conductivity is given by

$$\sigma = \lim_{\omega \to 0} \frac{a_{x-}}{i\omega a_{x+}}. \tag{24}$$

As a holographic application of the membrane paradigm of black holes, we can directly obtain the dc conductivity from Eq. 21 using the method proposed by Iqbal and Liu in Ref. [48]. In fact, the transport coefficients in the dual field theory can be obtained from the horizon geometry of the dual gravity in the low-frequency limit. Applying this to the $U(1)$ gauge field, this conclusion implies that the dc conductivity is given by the coefficient of the gauge field kinetic term evaluated at the horizon. To see this, we assume that $T > 0$ and $\omega \to 0$, and then we can neglect all the terms of ω in Eqs. 21. We first note that

$$\begin{aligned} \lim_{r\to\infty} r^{z+1}f(r)(a_x' - \lambda^2 C_{rx}/4) &= r^{z+1}z\left(\frac{-\langle J_x\rangle}{r^{z+1}} + \frac{\lambda^2\langle J_x\rangle}{4r^{z+1}m^2}\right) \\ &= -z(1-\lambda^2/4m^2)\langle J_x\rangle. \end{aligned} \tag{25}$$

Equation (21c) shows that this quantity is conserved along the direction r. So, at the horizon, using Eqs. (21b) and (21c), we have

$$\begin{aligned} &-z(1-\lambda^2/4m^2)\langle J_x\rangle \\ &\quad = \lim_{r\to 1} r^{z+1} f(a_x' - \lambda^2 C_{rx}/4)|_{r=r_+}, \\ &\quad = r^{z+1}f\left[\left(1 - \frac{\lambda^2}{4m^2}\right)a_x' - \frac{\lambda^2 J p\rho C_{ty}}{m^2 f r^{2z+2}}\right]_{r=r_h}. \end{aligned} \tag{26}$$

Combining Eqs. (21a) with (21b) and considering the fact that C_{ty} is regular at the horizon, we have

$$\left[m^2 + \frac{16J^2p^2\rho^2}{m^2r^{2z+2}}\right]C_{ty} = -\frac{4Jp\rho}{m^2}fa_x' + (z-1)fC_{ty}' \tag{27}$$

at $r \to r_h^+$. Thus, we have from Eqs. (27) and (26) that

$$\begin{aligned} &-z(1-\lambda^2/4m^2)\langle J_x\rangle \\ &\quad = \lim_{r\to r_h^+} r^2 f a_x' \left(1 - \frac{\lambda^2}{4m^2}\right) \\ &\quad\quad \times \left[1 + \frac{4J^2p^2\rho^2\lambda^2}{(m^2 - \frac{\lambda^2}{4})(m^4 + 16J^2p^2\rho^2/r^{2z+2})}\right]. \end{aligned} \tag{28}$$

Now, let us take the ingoing condition for a_x at the horizon, which tells us that

$$r^{z+1}fa_x' = \frac{d}{dr_*}a_x = -i\omega a_x, \quad \text{at } r \to r_h^+; \tag{29}$$

finally, we get

$$\langle J_x\rangle = \frac{i\omega a_x(r_+)}{z}\left[1 + \frac{4J^2p_0^2\rho_0^2\lambda^2}{(m^2 - \frac{\lambda^2}{4})(m^4 + 16J^2p_0^2\rho_0^2/r_+^{2z+2})}\right]. \tag{30}$$

Here, p_0 and ρ_0 are the initial values of $p(r)$ and $\rho(r)$ at the horizon, which can be computed from Eq. (11). In the low-frequency limit, Eq. (21) implies that the electric field is constant, i.e., $\lim_{r=r_h} a_x(r) = a_{x+}$. It follows that we can obtain the dc conductivity near the horizon as

$$\sigma = \frac{1}{z}\left[1 + \frac{4Jp_0^2\rho_0^2\lambda^2}{(m^2 - \frac{\lambda^2}{4})(m^4 + 16J^2p_0^2\rho_0^2/r_h^{2z+2})}\right]. \tag{31}$$

With the appearance of ferromagnetism, dc resistivity decreases when the sample gets cooling, which shows in many interesting phenomena in condensed matter physics, especially in a class of manganese oxides which are widespread because of the discovery of CMR [49,50]. Note that this effect has a complete different physical origin from the "giant" magnetoresistance observed in layered and clustered compounds. In the last 20 years, CMR has been among the main topics of study within the area of strongly correlated electron systems, and its popularity is reaching the level comparable to that of the high-temperature

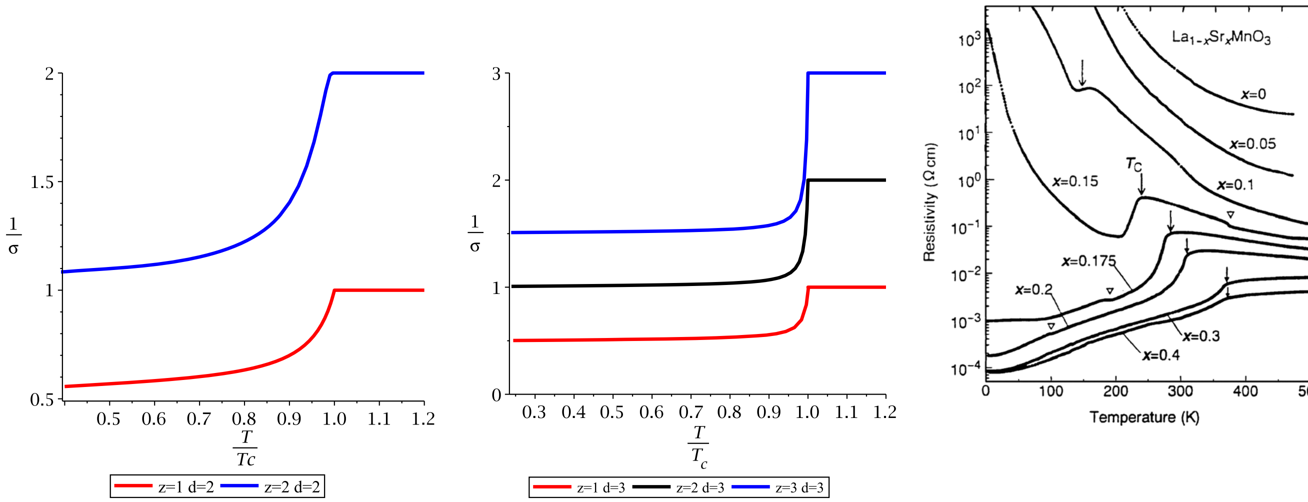

FIG. 3. Left panel: dc resistivity vs temperature in our model. Here, we choose parameters as $m^2 = -J = 1/8$ and $\lambda = 1/2$. Right panel: Temperature dependence of resistivity for various single crystals of $La_{1-x}Sr_xMnO_3$. Arrows indicate the Curie temperature. For more details, see Ref. [51].

superconducting cuprates. Here, the expression of Eq. (31) is just appropriate for the case of 4D spacetime. However, for the 5D Lifshitz spacetime, we only need to replace the coefficient $1/z$ in front of the bracket in Eq. (31) with $1/(z+1)$. It is not difficult to find that the dynamical exponent z has no effect on the shape of curve for the fixed D from Fig. 3, but it affects the value of dc resistivity when the sample gets cooling; i.e., the bigger the value of z, the bigger the dc resistivity, although it decreases with the lower temperature. Moreover, the dc resistivity decreases faster near the critical temperature T_c in the case of 5D than the in the case of 4D. In the right panel of Fig. 3, we show the experimental data from a typical CMR material $La_{1-x}Sr_xMnO_3$ as an example. We see that our model gives a very similar behavior to the latter in a composition range of $x \geq 0.175$. Meanwhile, Fig. 3 shows that the effect of dynamical exponent z on dc resistivity is different from the composition x; i.e., the increase of the composition x will result in the decrease of dc resistivity. Of course, we should mention here that there still exist some differences between our model result and experimental data on CMR. In general, when $T > T_c$, the material shows a semiconductor or insulator behavior, and the dc resistivity increases with cooling the sample which has been realized by introducing a massive 2-form field and a dilaton field coupled with the U(1) gauge field in the asymptotic AdS black brane background [30]. In our model, however, the dc resistivity is a constant when $T > T_c$, which is similar to the Ref. [34]. So this model only gives partial property of CMR when $T < T_c$. But this is an exciting and enlightening result because it implies that this model still can lead to a possibility to build a holographic CMR model in the Lifshitz black hole and to investigate this typical and important strong correlated electrons system in the AdS/CFT setup.

III. SEMIANALYTIC CALCULATIONS NEAR THE CRITICAL TEMPERATURE

In this section, to complement the numerical calculations, we study the magnetic moment and static magnetic susceptibility by using the semianalytic method, which is different from the analytic method in holographic superconductors, but it seems more accurate. Now, we focus on the case of the four-dimensional Lifshitz black hole. It is convenient to make a coordinate transformation by $u = r_h/r$. As p can be solved directly, then we put it into the equation of $\rho(r)$ and get when $z \neq d$

$$\rho'' + \left(\frac{3-z}{u} + \frac{f'}{f}\right)\rho' - \left[\frac{m^2}{u^2 f} + \frac{4J\mu^2 u^2 (2-z)^2}{(m^2 - 4J\rho^2 u^4)^2 f}\right]\rho + \frac{B}{u^2 f} = 0. \tag{32}$$

As we will care about the behavior of $T \to T_c$, the value of ρ will be a small quantity near the transition point. In this case, we can make a Taylor expansion on the nonlinear term of ρ in Eq. (32) as

$$\frac{4J\mu^2 u^2 (2-z)^2}{(m^2 - 4J\rho^2 u^4)^2} = \frac{4J\mu^2 u^2 (2-z)^2}{m^4} + \frac{32 J^2 \mu^2 \rho^2 u^6 (2-z)^6}{m^6} + \mathcal{O}(\rho^4). \tag{33}$$

Note that for the case of $z = d$ all the terms about $(2-z)$ in molecules will be replaced by 1, and some expressions in the following will also be changed. Here, we do not talk about it in detail. When neglecting the high-order terms, Eq. (32) can be rewritten as

$$\hat{L}\rho = \tilde{J}_f\rho^3 u^{9-z} + Bu^{1-z},$$
$$\hat{L} = -\frac{d}{dz}\left[u^{3-z}f(u)\frac{d}{du}\right] + q(u),$$
$$q(u) = m^2u^{1-z} + \frac{4J\mu^2u^{5-z}(2-z)^2}{m^4},$$
$$\tilde{J}_f = -32J^2\mu^2(2-z)^6/m^6 < 0. \quad (34)$$

Up to the order of ρ^4, the part of the polarization field in action (7) can be written as

$$\frac{S(T,B;\rho)}{\lambda^2V_2} = \left(\frac{u^{3-z}}{2}f\rho'\rho + u^{2-z}f\rho^2\right)\Big|_0^{z_h} - \int_0^{u_h}dz\left[\frac{\rho}{2}\hat{L}\rho + B\rho u^{1-z} - \frac{\tilde{J}_f}{4}u^{9-z}\rho^4\right], \quad (35)$$

which is a function of T and B but a functional of ρ. The asymptotic solution for Eq. (34) is

$$\rho = \tilde{\rho} + \frac{B}{m^2}, \quad \text{with} \quad \tilde{\rho} = \rho_+u^{\Delta_-} + \rho_-u^{\Delta_+}. \quad (36)$$

The source free condition is $\rho_+ = 0$ as $u \to 0^+$. Under this, the grand thermodynamic potential or free energy in the grand canonical ensemble Ω is

$$\Omega(T,B;\rho) = \tilde{\Omega}(T,B;\rho)V_2 = \lambda^2V_2\int_0^{u_h}dz\left[\frac{\rho}{2}\hat{L}\rho + B\rho u^{1-z} - \frac{\tilde{J}_f}{4}u^{9-z}\rho^4\right]. \quad (37)$$

According to the thermodynamic relationship,

$$d\Omega(T,B) = -SdT - V_2NdB \Rightarrow N = -\frac{1}{V_2}\left(\frac{\partial\Omega(T,B)}{\partial B}\right)_T. \quad (38)$$

It seems that the magnetic moment should be

$$N = -\frac{1}{V_2}\left(\frac{\partial\Omega(T,B;\rho)}{\partial B}\right)_{T,\rho} = -\lambda^2\int_0^{u_h}\rho u^{1-z}du. \quad (39)$$

However, comparing this result with the previous definition of the magnetic moment,

$$N/\lambda^2 = -\int_0^{u_h}\frac{\rho u^{1-z}}{2}du. \quad (40)$$

We find the difference factor 1/2 between Eq. (39) and (40). It should be shown that the expression (39) is not true. The reason has been explained in Ref. [34] according to the Euler homogenous function theorem and the scaling transformation. Therefore, we can get the definition (40) and still use it in the following. The key step for computing the grand thermodynamic potential is to structure the Sturm-Liouville problem,[1] which is the ordinary differential equation (ODE)

$$\hat{P}\rho_n = \frac{\hat{L}\rho_n}{\omega(u)} = \frac{1}{\omega(u)}\left\{-\frac{d}{du}\left[u^{3-z}f(u)\frac{d}{du}\right] + q(u)\right\}\rho_n = \lambda_n\rho_n, \quad (41)$$

with the boundary conditions; one is $|\rho_n(u_h)|$, required to be finite at $u = u_h$, $f(u_h) = 0$, and the other is $\rho_n(0) = 0$ at $u \to 0^+$. The weight function $\omega(u)$ can be an arbitrary positive continuous function in the region of $[0, u_h]$. From a practical point of view, we choose the weight function such that the values of λ_n will not influence the asymptotic solutions of Eq. (41). There are many choices for the weight function. Here, we choose $\omega(r) = u^k$ with an integer $k > 2$.

When $r \to \infty$, we note that the asymptotic solution for Eq. (41) is

$$\rho_n = \rho_+u^{\Delta_-} + \rho_-u^{\Delta_+}. \quad (42)$$

One can find that the second boundary condition corresponds to $\rho_+ = 0$. Let $\mathcal{L}^2([0,u_h],\omega(u),du)$ be the Hilbert space of square integrable functions on $[0,u_h]$, i.e.,

$$\mathcal{L}^2([0,u_h],\omega(u),du) = \left\{h:[0,u_h]\mapsto\mathbb{R}\,\Big|\int_0^{u_h}\omega(u)|h(u)|^2du < \infty\right\}, \quad (43)$$

with the inner product

$$\langle h_1,h_2\rangle = \int_0^{u_h}\omega(u)h_1(u)h_2(u)du, \quad (44)$$

and D be the subspace of $\mathcal{L}^2([0,u_h],\omega(u),du)$ that satisfies the both of the boundary conditions, i.e.,

$$D = \{\forall\ h \in \mathcal{L}^2([0,u_h],\omega(u),du)|h \in C^2[0,u_h], h(0) = 0, |h(u_h)| < \infty\}. \quad (45)$$

Then, we can prove that $\hat{P}$ is the self-adjoint operator on D, i.e.,

[1] The method is similar to the one used in Ref. [52] but is completely different from the Sturm-Liouville eigenvalue method in Ref. [16]; there, the precision depends on the trial function one chooses.

$$\forall h_1, \quad h_2 \in D, \quad \langle h_1, \hat{P} h_2 \rangle = \langle \hat{P} h_1, h_2 \rangle. \tag{46}$$

According to the properties of Sturm-Liouville (SL) problem, the solutions of Eq. (41) form a function basis on D with which one can expand any functions belonging to D, i.e.,

$$\langle \rho_n, \rho_k \rangle = \delta_{nk}, \tag{47}$$

and

$$\forall h \in D, \quad \exists \{c_n\} \subset \mathbb{R}, h(u) = \sum_{n=1}^{\infty} c_n \rho_n(u) \tag{48}$$

with $c_n = \langle \rho_n, h \rangle$.

Let us now turn our attention to the free energy (37). For convenience, we will use scaling transformation to set $u_h = 1$ in the process of computation and then transform into the case of fixing charge density in the final results.

Let $\tilde{\rho}(r) = \rho(r) - B/m^2$ be any function configuration belonging to D, in which $\rho(r)$ does not need to be the solution of the EoM (34). We can use the eigenfunction ρ_n to expand $\tilde{\rho}(r)$ and theh magnetic moment as

$$\tilde{\rho} = \sum_{n=1}^{\infty} c_n \rho_n \Leftrightarrow \rho = \sum_{n=1}^{\infty} c_n \rho_n + \frac{B}{m^2}, \tag{49}$$

$$\begin{aligned} N &= -\int_0^1 \frac{\lambda^2 B u^{1-z}}{2m^2} du - \lambda^2 \int_0^1 \frac{\tilde{\rho} u^{1-z}}{2} du \\ &= -\int_0^1 \frac{\lambda^2 B u^{1-z}}{2m^2} du - \frac{\lambda^2}{2} \sum_{n=1}^{\infty} c_n N_n, \end{aligned} \tag{50}$$

where c_n and N_n are coefficients, defined as

$$c_n = \int_0^1 \omega \tilde{\rho} \rho_n du, \qquad N_n = \int_0^1 \rho_n u^{1-z} du. \tag{51}$$

Let us consider the case of spontaneous magnetization, i.e., the case with $B = 0$. In this case, we have

$$\tilde{\Omega}(T, c_n) = \lambda^2 \int_0^1 du \left[\frac{\omega \rho}{2} \hat{P} \rho - \tilde{J}_f u^{9-z} \rho^4 / 4 \right], \tag{52}$$

with $\rho = \sum_{n=1}^{\infty} c_n \rho_n$. Using the orthogonal relationship, we have

$$\begin{aligned} \tilde{\Omega}(T, c_n) &= \frac{\lambda^2}{2} \langle \rho, \hat{P} \rho \rangle - \frac{\lambda^2 \tilde{J}_f}{4} \int_0^1 u^{9-z} \rho^4 du \\ &= \frac{\lambda^2}{2} \sum_{n=1}^{\infty} \lambda_n c_n^2 - \frac{\lambda^2 \tilde{J}_f}{4} \int_0^1 u^{9-z} \rho^4 du. \end{aligned} \tag{53}$$

It follows that the nonzero solution appears only when $\lambda_1 < 0$, i.e., $T < T_c$. Because of $J < 0$, we can find that $\tilde{\Omega}(T, c_n) \geq 0$. The minimization of $\Omega(T, c_n) = 0$ is achieved only when $c_n = 0$, i.e., $\rho = 0$.

When $T \to T_c^-$, we can set $\lambda_1 = a_0 (T/T_c - 1)$ with $a_0 > 0$ and assume that the off-shell solution is dominated by the first term in Eq. (49) only, i.e., $|c_1| \gg c_n$ for $n \geq 2$ in Eq. (51). As a result, we have

$$\begin{aligned} \lambda^{-2} \tilde{\Omega}(T, c_n) &\simeq \frac{1}{2} \lambda_1 c_1^2 - \frac{\tilde{J}_f c_1^4}{4} \int_0^1 dz \rho_1^4 u^{9-z}, \\ &\simeq \frac{1}{2} a_0 (T/T_c - 1) c_1^2 - \tilde{J}_f c_1^4 a_1 \end{aligned} \tag{54}$$

with $a_1 = \frac{1}{4} \int_0^1 \rho_1^4 u^{9-z} du|_{T=T_c} > 0$ and

$$N \simeq -\lambda^2 c_1 N_1 / 2. \tag{55}$$

Putting Eq. (55) into Eq. (54), we can obtain

$$\begin{aligned} \tilde{\Omega}(T, c_n) &\simeq \tilde{\Omega}(T, N) \\ &\simeq \frac{2a_0}{\lambda^2 N_1^2} (T/T_c - 1) N^2 + \frac{-16 \tilde{J}_f a_1}{\lambda^6 N_1^4} N^4. \end{aligned} \tag{56}$$

It easy to see that this is just the Ginzburg-Landau theory of the ferromagnetic model. Based on the grand thermodynamic potential in Eq. (56), we can obtain the expression of the magnetic moment in the ferromagnetic phase as

$$N/\lambda^2 = \sqrt{\frac{N_1^2 a_0}{-16 \tilde{J}_f a_1}} (1 - T/T_c)^{1/2}. \tag{57}$$

This just confirms the critical behavior obtained in the numerical calculations, and the critical exponent $1/2$ is an exact result. In that follows, we will compute all the coefficients appearing in Eq. (57) and compare them with the numerical ones.

A. Spontaneous magnetization

Let us first compute N_1 and a_1. For this, we have to first find the eigenfunction ρ_1, which is the solution of

$$-\frac{d}{du} \left[u^{3-z} f(u) \frac{d\rho_n}{du} \right] + q(u) \rho_n = 0 \tag{58}$$

at $T = T_c$ with the conditions

$$\rho_1(1) = 1, \qquad \rho_{1+} = 0. \tag{59}$$

For convenience, here, we do not assume that $\{\rho_n\}$ form a unit base. Thus, we have

$$N_1 = \frac{1}{C_1} \int_0^1 \rho_1 u^{1-z} du, \quad a_1 = \frac{1}{4C_1^4} \int_0^1 u^{9-z} \rho_1^4 du, \tag{60}$$

where C_1 is the normalization coefficient and

$$C_1^2 = \langle \rho_1, \rho_1 \rangle = \int_0^1 \omega \rho_1^2 du. \quad (61)$$

We have

$$N^2/\mu_c^2 = \frac{N_1^2 a_0}{-16\tilde{J}_f a_1 \mu_c^2}(1 - T/T_c) \simeq a_2(1 - T/T_c). \quad (62)$$

To clarify that the results are independent of the specific form of the weight function, we choose $k = 3$, 4 as two examples. From Table I, we see that different weight functions give different values for N_1, a_1, and a_0 but the same value for the magnetic moment N (up to a numerical error).

The value of a_0 can also be obtained directly by solving the ODE (41). In the region near the critical temperature, we assume $\lambda_1 = a_0(T/T_c - 1)$. Note that all quantities in Eq. (41) are the functions of temperature; thus, taking the derivative with respect to T and evaluating at $T = T_c$, we get

$$\frac{d\hat{P}}{dT}\rho_1 + \hat{P}\frac{d\rho_1}{dT} = \frac{a_0}{T_c}\rho_1. \quad (63)$$

Here, ρ_1 is the eigenfunction of Eq. (58). Now, treat $\rho_T = \frac{d\rho_1}{dT}$ as an unknown function to be solved; then, the task to find a_0 becomes solving a nonhomogenous eigenvalue problem,

$$\hat{P}\rho_T = \left[\frac{a_0}{T_c} - \frac{d\hat{P}}{dT}\right]\rho_1. \quad (64)$$

At the AdS boundary, ρ_T has the same asymptotic behavior as Eq. (42), and thus we can impose the boundary conditions as

$$|\rho_T(1)| < \infty, \qquad \rho_{T+} = 0. \quad (65)$$

We find that $\rho_T \in D$. We then use the basis $\{\rho_n\}$ to expand ρ_T, i.e.,

$$\rho_T = \sum_{n=1}^{\infty} \frac{d_n}{C_n}\rho_n. \quad (66)$$

Here, C_n are the modules of ρ_n. Using the fact that $\lambda_1 = 0$ at $T = T_c$ and

$$\begin{aligned}\langle C_1^{-1}\rho_1, \hat{P}\rho_T \rangle &= \sum_{n=1}^{\infty} d_n \langle C_1^{-1}\rho_1, C_n^{-1}\hat{P}\rho_n \rangle \\ &= \sum_{n=1}^{\infty} d_n \lambda_n \delta_{1n} = d_1\lambda_1 = 0, \end{aligned} \quad (67)$$

we have

$$\begin{aligned}\left\langle \rho_1, \left[\frac{a_0}{T_c} - \frac{d\hat{P}}{dT}\right]\rho_1 \right\rangle &= \frac{a_0 C_1^2}{T_c} - \int_0^1 \omega\rho_1 \frac{d\hat{P}}{dT}\rho_1 dz \\ &= \frac{a_0 C_1^2}{T_c} - \int_0^1 \rho_1 \frac{d\hat{L}}{dT}\rho_1 du = 0. \end{aligned} \quad (68)$$

Furthermore, we get

$$a_0 = \frac{T_c}{C_1^2}\int_0^1 dz \rho_1 \frac{d\hat{L}}{dT}\rho_1. \quad (69)$$

This expression is valid in a canonical ensemble with fixed charge density $\sigma = 1$. It is very useful to find its equivalent form in the case with fixed $r_h = 1$, since it is convenient when we perform numerical computation. If we fix $r_h = 1$, the shooting parameter is the chemical potential μ. The relation between the temperature in the canonical ensemble and the charge density is given by

$$T = \frac{z+2}{4\pi\sigma^{z/2}}. \quad (70)$$

Thus, the expression (69) can be rewritten as

$$\begin{aligned} a_0 &= \frac{T_c}{C_1^2}\frac{d\mu}{dT}\int_0^1 du \rho_1 \frac{d\hat{L}}{d\mu}\rho_1 \\ &= -\frac{4\mu_c^3 \pi T_c}{(2+z)C_1^2}\int_0^1 du \rho_1 \frac{d\hat{L}}{d\mu}\rho_1 \bigg|_{\mu=\mu_c}. \end{aligned} \quad (71)$$

B. Susceptibility

When $B \neq 0$, the susceptibility for $T > T_c$ is defined as

$$\chi = \lim_{B\to 0}\left(\frac{\partial N}{\partial B}\right)_T. \quad (72)$$

In the case with $T > T_c$ and $B \to 0$, we can neglect the nonlinear term, i.e., setting $\tilde{J}_f = 0$. The solution of Eq. (34) can be expressed as

$$\rho = \sum_{n=1}^{\infty} c_n \rho_n + \frac{B}{m^2}. \quad (73)$$

Taking into account Eq. (34) with $\tilde{J}_f = 0$, we have

$$\begin{aligned} 0 = \hat{L}\rho - Bu^{1-z} &= \sum_{l=1}^{\infty} c_l \hat{L}\rho_l + \frac{4BJ\mu^2 u^{5-z}(2-z)^2}{m^6} \\ &= \sum_{l=1}^{\infty} c_l C_l^{-1}\lambda_l \omega \rho_l - \frac{4BJ\mu^2 z^4}{m^6}. \end{aligned} \quad (74)$$

Multiplying a factor ρ_n/C_n and integrating the above equation from 0 to 1, we can obtain

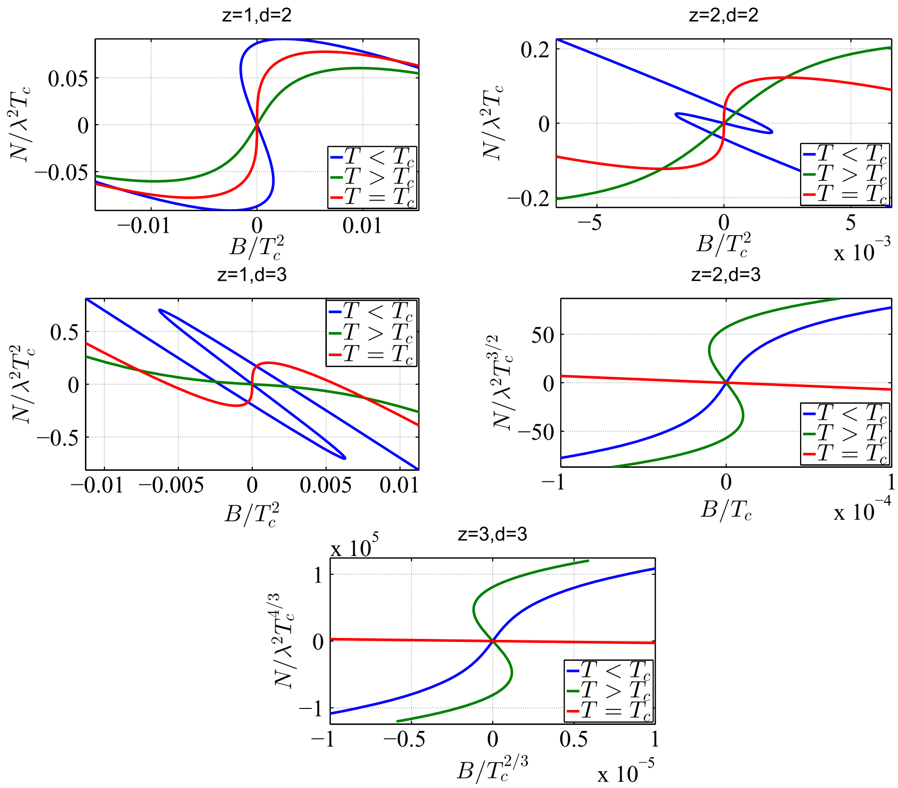

FIG. 4. The relation between the magnetic moment density N and external magnetic field B in the cases of $T = 1.05Tc$, $T = 0.9T_c$, and $T = T_c$, respectively

$$c_n = -\frac{B\gamma_n}{\lambda_n}, \quad \text{with} \quad \gamma_n = \int_0^1 \frac{4J\mu^2 u^{5-z}(2-z)^2}{C_n m^6}\rho_n du. \tag{75}$$

Thus, we can get the magnetic moment density as

$$N/\lambda^2 = -\int_0^1 \frac{Bu^{1-z}}{2m^2}du + B\sum_{n=1}^{\infty}\frac{\gamma_n N_n}{2\lambda_n} \tag{76}$$

and the magnetic susceptibility

$$\chi/\lambda^2 = -\int_0^1 \frac{u^{1-z}}{2m^2}du - \sum_{n=1}^{\infty}\frac{\gamma_n N_n}{2\lambda_n}. \tag{77}$$

When $T \to T_c^+$, we have $\lambda_1 = a_0(T/T_c - 1) \to 0^+$. Thus, χ is dominated by the first term in the summation of Eq. (77), and its inverse can be expressed as

$$\lambda^2\chi^{-1}/\mu_c^{\frac{2-z}{2}} = \frac{2a_0}{\mu_c^{\frac{2-z}{2}}}\gamma_1 N_1(T/T_c - 1), \quad \text{as } T \to T_c^+. \tag{78}$$

In the case of $m^2 = -J = 1/8$, for example, we have $\lambda^2\chi^{-1}/\mu_c \simeq 2.996(T/T_c - 1)$, which is very close to our numerical result $\lambda^2\chi^{-1}/\mu_c \simeq 2.966(T/T_c - 1)$ given in the numerical calculation when we take $z = 1$ in the case of 4D spacetime. But from Table I, it easy to see that the magnetic moment and susceptibility have a great gap when we compare the analytical method with numerical calculation, especially for the case of 5D Lifshitz spacetime.

Below, let us move to the case with $B \neq 0$. In this case, from Eq. (34), we have

$$\int_0^1 \rho_n(\omega\hat{P}\rho - Bu^{1-z} - \tilde{J}_f\rho^3 u^{9-z})du = 0. \tag{79}$$

According to Eq. (49), we can rewrite it as

$$\int_0^1 \rho_n\left(\omega\hat{P}\tilde{\rho} - B\left[u^{1-z} - \frac{q(u)}{m^2}\right] - \tilde{J}_f\rho^3 u^{9-z}\right)du = 0. \tag{80}$$

Using the expansion expression (49), we have

$$c_n C_n^2\lambda_n + B\gamma_n - \int_0^1 \rho_n\tilde{J}_f\rho^3 u^{9-z}du = 0, \quad n = 1, 2, \ldots. \tag{81}$$

For convenience, we assume that $\{\rho_n\}$ is a unit base, i.e., $C_n = 1$. Equation (81) is equivalent to Eq. (34) if we take all the terms in Eq. (49) into account. In the case of $T \to T_c^-$, assuming that the first term in Eq. (49) dominates only, i.e., $|c_1| \gg c_n$ for $n \geq 2$ in Eq. (51), we get

$$N/\lambda^2 = -\frac{B}{2m^2}\int_0^1 u^{1-z}du - c_1 N_1/2. \tag{82}$$

Taking $n = 1$ in Eq. (81), we have

$$c_1\lambda_1 + B\gamma_1 - c_1^3\tilde{J}_f \int_0^1 \rho_1^4 u^{9-z}du = c_1\lambda_1 + B\gamma_1 - 4c_1^3\tilde{J}_f a_1 = 0. \tag{83}$$

For a given temperature $T \to T_c$, we can combine Eq. (82) with Eq. (83) to obtain a relation between the external magnetic field B and magnetic moment N. Figure 4 shows the results with $T = 1.05T_c$, $T = 0.9T_c$, and $T = T_c$, respectively, in the case of $m^2 = -J = 1/8$. We see that it is very similar to what we have obtained in Ref. [34], particularly for the case of $z = 1$, $d = 2$. In the case of $T < T_c$, when the external field continuously changes between $-B_{\max}$ and $B_{\max}$ periodically, the metastable states of the magnetic moment can appear. Thus, we see a hysteresis loop in the single magnetic domain. Furthermore, from Fig. 4, it is easy to see that the magnetic moment is not single valued with a general z and D, and the Lifshitz dynamical exponent z has an effect on the hysteresis loop quantitatively. Particularly, for the cases of $z = 2$ in 4D and $z = 3$ in 5D spacetime, the period of the external field B is shorter, and the value of the magnetic moment N will become bigger than the ones for the cases of other z in 4D and 5D spacetime. The reason for this phenomenon is that the critical temperature T_c increases with increasing z. It makes the phase transition happen easily. In other words, the magnetic moment N is more likely to arrive at a certain value with the effect of dynamical exponent z. At the same time, it means one just needs a smaller external magnetic field to realize the hysteresis loop.

IV. SUMMARY AND DISCUSSION

In summary, we have numerically and analytically investigated the holographic paramagnetism-ferromagnetism phase transition model in the 4D and 5D Lifshitz black holes in the probe limit by introducing a massive 2-form field coupled to the background Maxwell field and obtained the effects of the dynamical exponent z on the holographic paramagnetism-ferromagnetism phase transition. Our results are concluded as follows.

We have obtained the critical temperature T_c first if the model parameters are in some suitable region and then typically plotted the magnetic moment and the inverse susceptibility density as a function of the temperature. The results show that, in the case without an external magnetic field, the improving of the dynamical exponent z results in the increase of T_c, which implies that the increasing anisotropy between space and time enhances the phase transition. Especially, for the case of 5D Lifshitz spacetime, the value of the magnetic moment changes obviously compared with the 4D spacetime. In the vicinity of the critical point, however, the behavior of the magnetic moment is always as $\sim(1 - T/T_c)^{1/2}$, regardless of the values of z and D, which is in agreement with the result from mean field theory. And the dc resistivity is not relevant to the dynamical exponent z qualitatively, though in this probe limit, it is suppressed by spontaneous magnetization and shows a metallic behavior. But the value of dc resistivity is influenced when the sample gets cooling; i.e., the bigger the value of z, the bigger the dc resistivity, although it decreases with the decreasing temperature. Moreover, in the presence of the external magnetic field, the inverse magnetic susceptibility near the critical point behaves as $\sim(T/T_c - 1)$ in all cases, which satisfies the Cure-Weiss law.

Furthermore, by a semianalytic method, we have calculated the magnetic moment and static magnetic susceptibility and obtained the relation between external magnetic field B and magnetic moment N near the critical temperature. And we have observed the hysteresis loop in the single magnetic domain when the external field continuously changes between the maximum and minimum values periodically with a general z or D. But for the fixed value of D, the increase of the dynamical exponent z could result in shortening the period of the external magnetic field. In addition, the transformation period is smaller in the 5D case than in the 4D case.

Note that in this paper we only worked on the probe limit by neglecting the backreaction of the matter fields. Although the probe limit can reveal some significant properties of the holographic ferromagnetic phase transition, maybe the order of the phase transition could be changed once the backreaction is taken into consideration, and some new phases could emerge. Therefore, it is interesting to study the influence of the backreaction of the matter field to the Lifshitz background and to see whether there are some new features beyond the probe limit, which will be our research work in the near future.

ACKNOWLEDGMENTS

We would like to thank Prof. R. G. Cai and Dr. R. Q. Yang for their helpful discussions and comments. This work is supported by the National Natural Science Foundation of China (Grants No. 11175077 and No. 11575075) and the Joint Specialized Research Fund for the Doctoral Program of Higher Education, Ministry of Education, China (Grant No. 20122136110002).

[1] J. M. Maldacena, The large N limit of superconformal field theories and supergravity, Int. J. Theor. Phys. **38**, 1113 (1999); Adv. Theor. Math. Phys. **2**, 231 (1998).
[2] S. S. Gubser, I. R. Klebanov, and A. M. Polyakov, Gauge theory correlators from noncritical string theory, Phys. Lett. B **428**, 105 (1998).
[3] E. Witten, Anti-de Sitter space and holography, Adv. Theor. Math. Phys. **2**, 253 (1998).
[4] E. Witten, Anti-de Sitter space, thermal phase transition, and confinement in gauge theories, Adv. Theor. Math. Phys. **2**, 505 (1998).
[5] S. A. Hartnoll, Lectures on holographic methods for condensed matter physics, Classical Quantum Gravity **26**, 224002 (2009).
[6] C. P. Herzog, Lectures on holographic superfluidity and superconductivity, J. Phys. A **42**, 343001 (2009).
[7] J. McGreevy, Holographic duality with a view toward many-body physics, Adv. High Energy Phys. **2010**, 723105 (2010).
[8] S. Sachdev, Condensed matter and AdS/CFT, Lect. Notes Phys. **828**, 273 (2011).
[9] S. A. Hartnoll, C. P. Herzog, and G. T. Horowitz, Building a Holographic Superconductor, Phys. Rev. Lett. **101**, 031601 (2008).
[10] S. A. Hartnoll, C. P. Herzog, and G. T. Horowitz, Holographic superconductors, J. High Energy Phys. 12 (2008) 015.
[11] S. S. Gubser, Colorful Horizons with Charge in Anti-de Sitter Space, Phys. Rev. Lett. **101**, 191601 (2008).
[12] S. S. Gubser and S. S. Pufu, The gravity dual of a p-wave superconductor, J. High Energy Phys. 11 (2008) 033.
[13] G. T. Horowitz and M. M. Roberts, Holographic superconductors with various condensates, Phys. Rev. D **78**, 126008 (2008).
[14] G. T. Horowitz, Introduction to holographic superconductors, Lect. Notes Phys. **828**, 313 (2011).
[15] G. T. Horowitz and M. M. Roberts, Zero temperature limit of holographic superconductors, J. High Energy Phys. 11 (2009) 015.
[16] G. Siopsis and J. Therrien, Analytic calculation of properties of holographic superconductors, J. High Energy Phys. 05 (2010) 013.
[17] S. Nakamura, H. Ooguri, and C. S. Park, Gravity dual of spatially modulated phase, Phys. Rev. D **81**, 044018 (2010).
[18] A. Donos and J. P. Gauntlett, Holographic striped phases, J. High Energy Phys. 08 (2011) 140.
[19] G. T. Horowitz, J. E. Santos, and D. Tong, Optical conductivity with holographic lattices, J. High Energy Phys. 07 (2012) 168.
[20] Y. Ling, C. Niu, J. P. Wu, Z. Y. Xian, and H. b. Zhang, Holographic fermionic liquid with lattices, J. High Energy Phys. 07 (2013) 045.
[21] M. Rozali, D. Smyth, E. Sorkin, and J. B. Stang, Striped order in AdS/CFT correspondence, Phys. Rev. D **87**, 126007 (2013).
[22] R. G. Cai, Y. Q. Wang, and H. Q. Zhang, A holographic model of SQUID, J. High Energy Phys. 01 (2014) 039.
[23] K. Murata, S. Kinoshita, and N. Tanahashi, Non-equilibrium condensation process in a holographic superconductor, J. High Energy Phys. 07 (2010) 050.
[24] M. J. Bhaseen, J. P. Gauntlett, B. D. Simons, J. Sonner, and T. Wiseman, Holographic Superfluids and the Dynamics of Symmetry Breaking, Phys. Rev. Lett. **110**, 015301 (2013).
[25] A. Adams, P. M. Chesler, and H. Liu, Holographic vortex liquids and superfluid turbulence, Science **341**, 368 (2013).
[26] A. M. Garca-Garca, H. B. Zeng, and H. Q. Zhang, A thermal quench induces spatial inhomogeneities in a holographic superconductor, J. High Energy Phys. 07 (2014) 096.
[27] P. M. Chesler and L. G. Yaffe, Numerical solution of gravitational dynamics in asymptotically anti-de Sitter spacetimes, J. High Energy Phys. 07 (2014) 086.
[28] N. Iqbal, H. Liu, M. Mezei, and Q. Si, Quantum phase transitions in holographic models of magnetism and superconductors, Phys. Rev. D **82**, 045002 (2010).
[29] R. G. Cai and R. Q. Yang, Paramagnetism-ferromagnetism phase transition in a dyonic black hole, Phys. Rev. D **90**, 081901 (2014).
[30] R. G. Cai and R. Q. Yang, Antisymmetric tensor field and spontaneous magnetization in holographic duality, Phys. Rev. D **92**, 046001 (2015).
[31] R. G. Cai and R. Q. Yang, Holographic model for the paramagnetism/antiferromagnetism phase transition, Phys. Rev. D **91**, 086001 (2015).
[32] R. G. Cai and R. Q. Yang, Coexistence and competition of ferromagnetism and p-wave superconductivity in holographic model, Phys. Rev. D **91**, 026001 (2015).
[33] R. G. Cai and R. Q. Yang, Insulator/metal phase transition and colossal magnetoresistance in holographic model, Phys. Rev. D **92**, 106002 (2015).
[34] R. G. Cai, R. Q. Yang, Y. B. Wu, and C. Y. Zhang, Massive 2-form field and holographic ferromagnetic phase transition, J. High Energy Phys. 11 (2015) 021.
[35] N. Yokoi, M. Ishihara, K. Sato, and E. Saitoh, A holographic realization of ferromagnets, Phys. Rev. D **93**, 026002 (2016).
[36] S. Kachru, X. Liu, and M. Mulligan, Gravity duals of Lifshitz-like fixed points, Phys. Rev. D **78**, 106005 (2008).
[37] M. Taylor, Non-relativistic holography, arXiv:0812.0530.
[38] D. W. Pang, A note on black holes in asymptotically Lifshitz spacetime, Commun. Theor. Phys. **62**, 265 (2014).
[39] E. J. Brynjolfsson, U. H. Danielsson, L. Thorlacius, and T. Zingg, Holographic superconductors with Lifshitz scaling, J. Phys. A **43**, 065401 (2010).
[40] S. J. Sin, S. S. Xu, and Y. Zhou, Holographic superconductor for a Lifshitz fixed point, Int. J. Mod. Phys. A **26**, 4617 (2011).
[41] Y. Bu, Holographic superconductors with $z = 2$ Lifshitz scaling, Phys. Rev. D **86**, 046007 (2012).
[42] Z. Fan, Holographic superconductors with hyperscaling violation, J. High Energy Phys. 09 (2013) 048.
[43] E. Abdalla, J. de Oliveira, A. B. Pavan, and C. E. Pellicer, Holographic phase transition and conductivity in three dimensional Lifshitz black hole, arXiv:1307.1460.
[44] R. G. Cai and H. Q. Zhang, Holographic superconductors with Horava-Lifshitz black holes, Phys. Rev. D **81**, 066003 (2010).
[45] S. A. Hartnoll and R. Pourhasan, Entropy balance in holographic superconductors, J. High Energy Phys. 07 (2012) 114.
[46] Y. B. Wu, J. W. Lu, M. L. Liu, J. B. Lu, C. Y. Zhang, and Z. Q. Yang, Lifshitz effects on vector condensate induced by a magnetic field, Phys. Rev. D **89**, 106006 (2014).

[47] J. W. Lu, Y. B. Wu, P. Qian, Y. Y. Zhao, and X. Zhang, Lifshitz scaling effects on holographic superconductors, Nucl. Phys. **B887**, 112 (2014).
[48] N. Iqbal and H. Liu, Universality of the hydrodynamic limit in AdS/CFT and the membrane paradigm, Phys. Rev. D **79**, 025023 (2009).
[49] E. Dagottoa, T. Hotta, and A. Moreo, Colossal magneto-resistant materials: The key role of phase separation, Phys. Rep. **344**, 1 (2001).
[50] E. L. Nagaev, Colossal-magnetoresistance materials: Manganites and conventional ferromagnetic semiconductors, Phys. Rep. **346**, 387 (2001).
[51] A. Urushibara, Y. Moritomo, T. Arima, A. Asamitsu, G. Kido, and Y. Tokura, Insulator-metal transition and giant magnetoresistance in $La_{1-x}Sr_xMnO_3$, Phys. Rev. B **51**, 14103 (1995).
[52] L. Yin, D. Hou, and H. c. Ren, Ginzburg-Landau theory of a holographic superconductor, Phys. Rev. D **91**, 026003 (2015).